The illusion of diffusion: Field evidence for depth-dependent sediment transport

Arjun M. Heimsath* Department of Earth Sciences, Dartmouth College, Hanover, New Hampshire 03755, USA
David Jon Furbish Department of Earth and Environmental Sciences, Vanderbilt University, Nashville, Tennessee 37235, USA
William E. Dietrich Department of Earth and Planetary Sciences, University of California, Berkeley, California 94720, USA

ABSTRACT

Soil-covered upland landscapes are common in much of the habitable world, and our understanding of their evolution as a function of different climatic, tectonic, and geologic regimes is important across a wide range of disciplines. Erosion laws direct quantitative study of the processes shaping Earth's surface and form the basis of landscape evolution modeling, but are based on limited field data. Here we use in situ–produced cosmogenic ^{10}Be and ^{26}Al concentrations from granitic saprolite to quantify an exponential decline in soil production with increasing soil thickness for a new field site in Point Reyes, California. Results are similar to soil production functions from two different, previously studied field sites, and are used with extensive measurements of soil thickness to quantify depth-integrated sediment transport flux. Plots of calculated sediment fluxes against the product of soil depth and hillslope gradient provide the first field-based evidence that soil transport is a nonlinear, depth-dependent function. Data from all sites suggest that the widely used linear diffusion equation is only appropriate for shallow gradient, convex-up regions, while the depth-dependent transport law is more broadly applicable. Quantifying both the mobile soil thickness and landscape morphology is therefore critical to understanding how landscapes evolve.

Keywords: erosion, geomorphology, cosmogenic nuclides, landscape evolution, soil transport.

INTRODUCTION

Upland landscapes across a large part of Earth's surface are soil mantled. Erosional processes transport soil from these uplands into networks of stream channels, and ultimately into sediment sinks, but the mathematical relationships used to model these processes are based on limited field data (Dietrich et al., 2003; Furbish, 2003). The persistence of soil across the landscape depends in large part on the production of soil from the underlying bedrock at rates at least equal to the erosion rate (Anderson and Humphrey, 1989; Carson and Kirkby, 1972; Dietrich et al., 1995; Heimsath et al., 1997). Cosmogenic nuclide-based techniques determined soil production functions under different climatic, lithologic, and tectonic conditions (Heimsath et al., 1997, 2000), while field-based quantification of a soil transport function remains elusive (Dietrich et al., 2003).

Transport of soil is widely assumed to depend linearly on topographic slope, which results in a differential equation similar to the diffusion equation when used in continuity equations (e.g., Dietrich et al., 1995). There are, however, limited field data supporting a linear transport law, and its appeal rests with its mathematical simplicity rather than its process-based confirmation. The term diffusive refers not to the processes, but to how the land surface might be evolving. Other work (e.g., Andrews and Buckman, 1975) suggested that transport depends nonlinearly on slope, especially on steeper gradients, but the only direct measurements are from experimental modeling (Roering et al., 2001) and analyses of fire-induced dry ravel (Gabet, 2003; Roering and Gerber, 2005). Many workers have explored transport processes (e.g., Fleming and Johnson, 1975; Gabet, 2000; McKean et al., 1993), but field or measurement constraints often obscure the detailed processes of transport. Here we combine new cosmogenic nuclide-based soil production rates with topographic surveys and extensive measurements of soil depth across three different landscapes to provide the first field-based evidence of a nonlinear, depth-dependent transport function.

SOIL TRANSPORT MODELS

The conceptual framework used here is based on the equation of mass conservation for physically mobile soil overlying its parent material (Carson and Kirkby, 1972; Dietrich et al., 1995). Typically, the boundary between soil and the underlying weathered (or fresh) bedrock is abrupt and can be defined within a few centimeters. Soil is produced and transported by mechanical processes, and soil production rates decline exponentially with depth (Heimsath et al., 1997, 2000). The transition from soil-mantled to bedrock-dominated landscapes occurs when transport rates are greater than production rates (Anderson and Humphrey, 1989), and two transport functions are typically used to model landscape evolution (Dietrich et al., 2003). The slope-dependent transport law has its basis in the characteristic form of convex, soil-mantled landscapes assumed to be in equilibrium, and has some field support (e.g., McKean et al., 1993; Roering et al., 2002). A nonlinear, slope-dependent transport law also has its roots in morphometric observations, and has recent support with the veracity of assuming landscape equilibrium (Roering et al., 1999), experimental constraints (Roering et al., 2001), or postfire ravel (Gabet, 2003; Roering and Gerber, 2005).

Disturbances due to freeze-thaw (e.g., Anderson, 2002; Matsuoka and Moriwaki, 1992), shrink-swell (e.g., Fleming and Johnson, 1975), viscous or plastic flow (e.g., Ahnert, 1976), and biological activity (e.g. Gabet, 2000) cause soil transport, and the disturbances decline with depth, typically exponentially (e.g. Roering, 2004). Disturbance penetration distance sets the mobile soil thickness. In thin soils, the penetration is limited by underlying bedrock or saprolite, but can result in mechanical soil production from the rock. In thick soils, the disturbance-driven depth can be less than the thickness of the total deposit. This disturbance depth influence suggests that soil transport should depend on local gradient and mobile depth, and while depth-slope dependency has long been postulated (e.g. Ahnert, 1967), field data have been lacking.

Recently, two theories have been proposed (Furbish, 2003; Roering, 2004) that explicitly model transport due to biotic disturbance. Here we test the simpler of the two, as we lack data on the velocity profiles that would inform the Roering (2004) model. Furbish (2003) argues that the dilational effects of biotic activity cause the vertically averaged volumetric flux density (i.e., vertically averaged velocity), $\bar{q}_s$(L t^{-1}), to be proportional to land surface, z, gradient. The depth-integrated flux per unit contour distance is then the product of mobile soil thickness, H, and this flux density:

$$H\bar{q}_s = -K_h H \nabla_z. \quad (1)$$

The coefficient K_h (L t^{-1}) characterizes the magnitude and frequency of downslope soil-

*E-mail: Arjun.Heimsath@Dartmouth.edu.

particle motions. It is constant with uniform particle activity over depth, but may vary if particle activity declines significantly with depth wherein transport occurs mostly near the surface. For simplicity, here we assume vertically uniform particle activity/mixing as a first step in testing a depth-slope transport relation.

FIELD SITES AND METHODS

Each field site is a soil-mantled upland landscape with the characteristic convex form used to infer a slope-dependent transport law. The Nunnock River (NR), southeastern Australia, field site is at the base of the passive continental margin escarpment (Heimsath et al., 2000). Underlying bedrock is Late Silurian to Early Devonian granodiorite, rainfall is ~900 mm yr^{-1} distributed equally across seasons, and vegetation is a dry sclerophyll forest. We also use the well-studied region of Tennessee Valley, northern California, with a Mediterranean climate, active tectonic setting, and metasedimentary bedrock typical of the Franciscan Formation (e.g., Dietrich et al., 1995). Our third site is on the relatively steep slopes of Mount Vision, in Point Reyes, California, is underlain entirely by granitic rocks, mostly quartz diorite and granodiorite (Galloway, 1977), and is ~30 km north of the Tennessee Valley site. It is outside historical agricultural impacts and supports a native forest of Bishop pine trees that burns periodically and is replaced by grassland and scrub underbrush. Tree throw contributes to soil production and transport, which are also observed to be due to burrowing gophers, mountain beavers, and invertebrates, with overland flow potential following fires. Biogenic processes are also observed to be dominant at the Nunnock River and Tennessee Valley sites.

Soil production rates from parent material underlying the soil mantle, and erosion rates from exposed bedrock or stream sediments, can be quantified by measuring the in situ–produced cosmogenic nuclides, ^{10}Be and ^{26}Al. Measured concentrations of either nuclide depend on the nuclide production rate and half-life as well as the erosion or soil production rate of the target material. We use ^{10}Be and ^{26}Al concentrations from saprolite, bedrock, and stream sediments to determine soil production, tor erosion, and average erosion rates for each site, and report the new Point Reyes results here. Site-specific nuclide-derived soil production rates and detailed soil depth measurements are used to determine the depth-integrated flux for each site. Soil thickness is measured by digging soil pits to the soil-bedrock boundary at ~10 m intervals across the sites. We assume that on convex portions of the landscape, soil production and transport is much faster than the rate of change in topography. In this case, the rate of soil thickness change is sufficiently small that we determine soil flux by integrating soil production within flow tubes mapped from ridge crest to base (see Data Repository[1]).

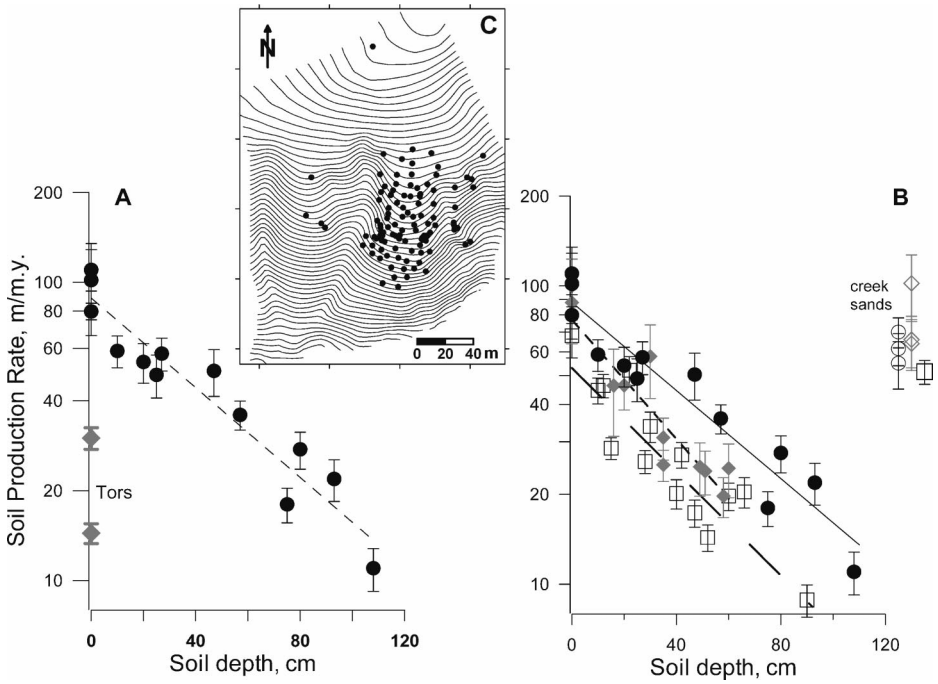

Figure 1. Soil production functions. A: Point Reyes (PR). Solid black circles are averages of rates from both ^{10}Be and ^{26}Al (Table DR1; see footnote 1), and error bars represent all errors propagated through nuclide calculations, i.e., uncertainty in atomic absorption, accelerator mass spectrometry, bulk density and soil depth measurements, and attenuation length of cosmic rays. Gray diamonds are erosion rates from outcropping tors on ridge crests. B: Point Reyes data shown with results from Nunnock River (open black squares, long-dashed regression line; Heimsath et al., 2000) and Tennessee Valley (gray diamonds, short-dashed regression line; Heimsath et al., 1997); open symbols labeled creek sands are average rates from detrital cosmogenic nuclide concentrations from each site. C: Topographic map, 2 m contour intervals by laser total station survey, showing soil pit locations for PR. Creek drains right to left at page bottom and elevation of crest is 195 m.

SEDIMENT PRODUCTION

Soil production rates from 13 samples from the bedrock-soil interface at Point Reyes (Table 1) define a clear exponential decline of soil production with soil depth such that the variance-weighted best-fit regression (Fig. 1A) is

$$\varepsilon(H) = (88 \pm 6)e^{-(0.017\pm0.001)H}, \quad (2)$$

where soil production, $\varepsilon(H)$, is in meters per million years and soil depth, H, is in centimeters. Average erosion rates, inferred from three samples of stream sand from the creek draining the study area, determine a basin-averaged rate of 62 m/m.y., similar to that of Tennessee Valley (Fig. 1B). Lower erosion rates from two tors at Point Reyes are consistent with granitic core-stone emergence shown at Nunnock River (Heimsath et al., 2000). Comparison of the soil production functions reveals remarkable similarity in form with relatively little scatter around the Point Reyes regression line (Fig. 1B). Similar to the Nunnock River and Tennessee Valley sites, these data, combined with the spatial variation of depth data from Figure 2A, show spatially variable rates of soil production, indicating a landscape out of long-term dynamic equilibrium. This is not surprising given the proximity of the San Andreas fault to the site, and the southern California origin of the Point Reyes peninsula (Galloway, 1977).

The Point Reyes results are evidence for the applicability of the soil production function as a transport relationship (cf. Dietrich et al., 2003) characterizing hilly, soil-mantled landscapes. Comparison of functions from these different sites offers the potential for untangling the connections between erosion rates, climate, and tectonics. The slope of the dependency of production rate on soil depth shows that in all three cases (Fig. 1B), the production rate is halved by a cover of 35 cm

[1]GSA Data Repository item 2005186, Appendix 1, obtaining soil flux, and Table DR1 is available online at www.geosociety.org/pubs/ft2005.htm, or on request from editing@geosociety.org or Documents Secretary, GSA, P.O. Box 9140, Boulder, CO 80301-9140, USA.

and reduced to a tenth by 115 cm, which is roughly the maximum soil depth found on ridges. Soil depth varies across the study sites, with thinnest soils on the narrow ridge crests, and thicker soils bordering unchanneled valleys (e.g. Heimsath et al., 1997, 2000). The soil production functions (Fig. 1B) imply that ground surface lowering is highest on ridge crests. This apparent topographic disequilibrium may be counteracted by periodic evacuation of the adjacent colluvial fills, setting up a transient upslope thinning of soils (Dietrich et al., 1995).

DEPTH-DEPENDENT TRANSPORT

Soil depths vary spatially across the divergent areas of the Point Reyes landscape such that topographic curvature declines exponentially with increasing soil thickness (Fig. 2A), although a linear decline similar to the other field sites cannot be ruled out (Fig. 2B). In the case of a simple slope-dependency of transport, curvature is a proxy for soil production (Heimsath et al., 1999), and the exponential decline of curvature with depth would support the soil production function defined by equation 2, assuming an independently documented (Reneau, 1988) linear diffusivity of 30 cm^2yr^{-1}. The clear linear (versus exponential) decline of curvature with increasing soil depths at Nunnock River suggested, however, that a linear slope-dependent transport model did not adequately capture the transport mechanisms, prompting modeling (Braun et al., 2001) and optically stimulated luminescence (Heimsath et al., 2002) studies highlighting the role of soil thickness in sediment transport.

Here we plot depth-integrated flux, determined by integrating soil production rates downslope (Data Repository; see footnote 1), against the depth-slope product across all field areas to test equation 1 (Fig. 3A). We observe strong linear increases of soil flux with increasing depth-slope product for both Nunnock River (NR) and Tennessee Valley (TV), but no such relationship at Point Reyes (PR), where a purely slope-dependent relationship is a better fit. Two observations might explain the failure of the depth-slope model at PR. First, the significantly greater soil depths for any given curvature value suggest that the frequency and magnitude of biotic penetration into the soil might be mediated differently than at NR and TV, and not be captured by a constant K_h. Second, the higher gradients on the lower slopes of PR suggest that shallow landsliding might be a dominant process.

Data from Nunnock River support equation 1 with a transport coefficient, K_h, equal to 0.55 cm yr^{-1}. Roughly equating this coefficient to the linear diffusivity with an average soil thickness for Nunnock River of 50 cm yields a coefficient of 28 cm^2yr^{-1}, compared to the 40 cm^2yr^{-1} reported by Heimsath et al. (2000). Reversing the process for the Tennessee Valley and Point Reyes data, which have independently determined linear diffusivities of 50 and 30 cm^2yr^{-1} (Reneau, 1988) and average soil thicknesses of 40 cm and 60 cm, yields depth-dependent transport coefficients, K_h, of 1.25 and 0.5 cm yr^{-1}, respectively. Using the data from Tennessee Valley and Point Reyes (Fig. 3A), K_h values of 1.2 and 0.4 cm yr^{-1} are determined.

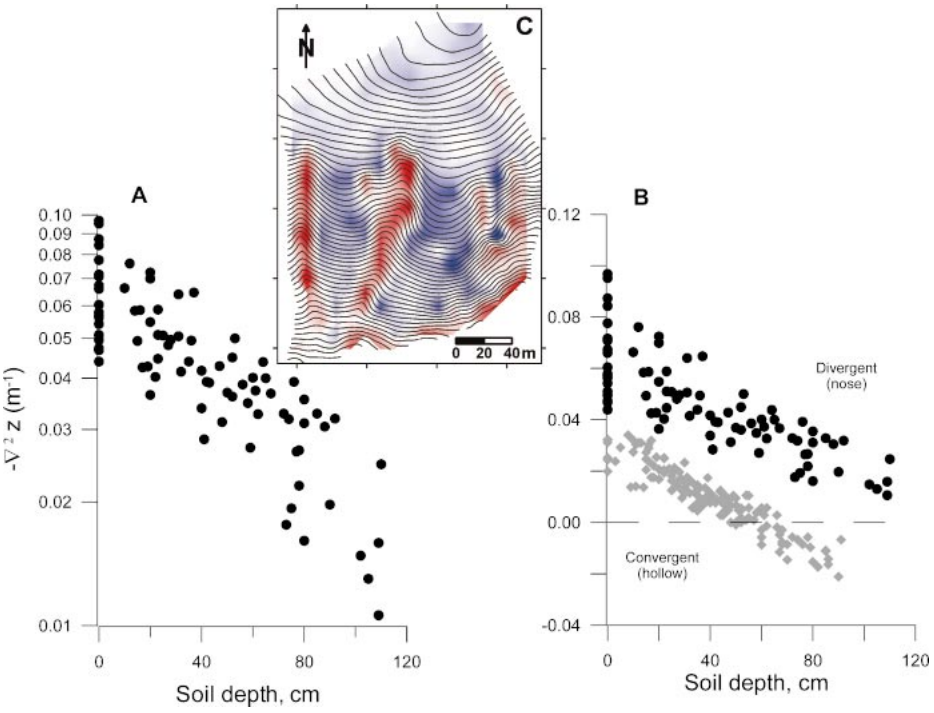

Figure 2. Negative curvature vs. vertical soil depth. Curvature calculated as in Heimsath et al. (1999) and is proxy for soil production if local soil depth is constant with time. A: Black circles from individual soil pits at Point Reyes with exponential negative curvature axis. B: Black circles (as in A) with open gray diamonds are from Nunnock River (Heimsath et al., 2000). Tennessee Valley data from Heimsath et al. (1997, 1999) overlay Nunnock River data values and range and are not included here for plot clarity. Black dashed line separates divergent from convergent topography. C: Curvature map for Point Reyes: blue represents convex and red represents concave topography.

This comparison of transport coefficients places the depth-dependent transport flux within the context of the more familiar slope-dependent transport framework and supports the applicability of a linear transport law for low-gradient convex landscapes. Plotting flux against gradient shows, however, that a linear relationship does not reflect all the data (Data Repository; see footnote 1). Our test for depth-dependent transport thus involves two sets of complementary plots: $H\bar{q_s}$ vs. HS (Fig. 3A) and $H\bar{q_s}$ $(HS)^{-1}$ versus downslope dis-

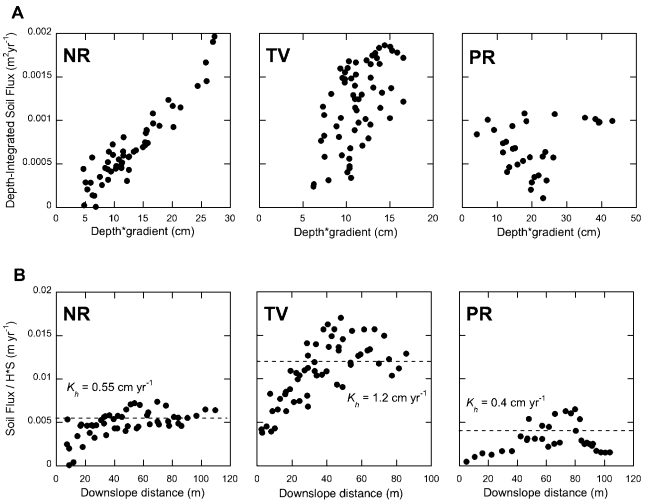

Figure 3. A: Depth-integrated soil flux (calculated as per Appendix 1; see footnote 1) per unit contour length (m^2yr^{-1}) vs. the depth-slope product (cm) for all field sites. B: Depth-integrated flux divided by depth-slope product vs. downslope distance. K_h value, determined by fitting data shown in A, is dashed line. NR—Nunnock River; TV—Tennessee Valley; PR—Point Reyes.

tance, X (Fig. 3B). If equation 1 is correct, the first plots (Fig. 3A) should show a linear increase, with slope equal to K_h and zero origin—in the absence of covariance of H or S with distance X. However, because $H\bar{q}_s$ must, by definition, increase with X, these plots might exhibit spurious covariance with the depth-slope product. Thus, the importance of the inset plots (Fig. 3B) is to remove any such covariance such that the data should be homoscedastic about a flat line equal to K_h (dashed line) to support equation 1. We observe, instead, an increase with distance close to the ridge crests, followed by a tendency to flatten roughly around the K_h values. Potential explanations for the increase include the unknown role of chemical weathering or a nonconstant covariant transport coefficient.

THE ILLUSION OF DIFFUSION

We present the first field-based test of the hypothesis that sediment transport is proportional to the product of soil depth and topographic gradient to support an alternative sediment transport law from the widely used diffusion model. To do this we quantify first a new soil production function based on cosmogenic nuclide analyses of bedrock beneath an actively eroding soil mantle. Soil production rates decline exponentially with soil depth across a broad spectrum of climate and tectonic regimes, supporting the function's generality as a geomorphic transport law. We then integrate downslope soil production rates using extensive field measurements of soil depth. Plotting depth-integrated flux against the depth-slope product shows support for a depth-dependent transport law at Nunnock River and Tennessee Valley, which have different bedrock, climate, and tectonic regimes. Although soil production and transport rates vary between sites, potentially driven by their respective tectonic and climatic settings, the forms of the transport functions are similar and may be driven by similarities in the biogenic processes. To further delimit soil transport will require quantifying soil and parent material chemical weathering, documenting velocity profiles, and extending analyses across the entire upland landscape. We conclude that it is an illusion to think of landscapes eroding by processes termed to be diffusive and suggest that future landscape evolution modeling efforts more completely couple spatial variations in soil depth with soil production and transport processes.

ACKNOWLEDGMENTS

We thank K. Heimsath and J. Roering for field assistance; S. Bateman, the landowner of the Nunnock River site; the National Park Service for access to Point Reyes; and the Golden Gate National Recreation Area for access to Tennessee Valley. M. Borosund helped with flow tube analyses. M Jungers, J. Roering, and an anonymous reviewer helped improve the paper. We were funded through the National Science Foundation. Nuclide measurements were partially performed under the auspices of the U.S. Department of Energy by Lawrence Livermore National Laboratory under contract W-7405-Eng-48.

REFERENCES CITED

Ahnert, F., 1967, The role of the equilibrium concept in the interpretation of landforms of fluvial erosion and deposition, *in* Macar, P., ed., L'evolution des versants: Liege, University of Liege, p. 23–41.

Ahnert, F., 1976, Brief description of a comprehensive three-dimensional process-response model of landform development: Zeitschrift fur Geomorphologie, supplement band, v. 25, p. 29–49.

Anderson, R.S., 2002, Modeling the tor-dotted crests, bedrock edges, and parabolic profiles of high alpine surfaces of the Wind River Range, Wyoming: Geomorphology, v. 46, p. 35–58.

Anderson, R.S., and Humphrey, N.F., 1989, Interaction of weathering and transport processes in the evolution of arid landscapes, *in* Cross, T.A., ed., Quantitative dynamic stratigraphy, Englewood cliffs, New Jersey, Prentice Hall, p. 349–361.

Andrews, D.J., and Buckman, R.C., 1975, Fitting degradation of shoreline scarps by a nonlinear diffusion model: Journal of Geophysical Research, v. 92, no. B12, p. 12,857–12,867.

Braun, J., Heimsath, A.M., and Chappell, J., 2001, Sediment transport mechanisms on soil-mantled hillslopes: Geology, v. 29, p. 683–686.

Carson, M.A., and Kirkby, M.J., 1972, Hillslope form and process: New York, Cambridge University Press, 475 p.

Dietrich, W.E., Reiss, R., Hsu, M.-L., and Montgomery, D.R., 1995, A process-based model for colluvial soil depth and shallow landsliding using digital elevation data: Hydrological Processes, v. 9, p. 383–400.

Dietrich, W.E., Bellugi, D., Heimsath, A.M., Roering, J.J., Sklar, L., and Stock, J.D., 2003, Geomorphic transport laws for predicting landscape form and dynamics, *in* Wilcock, P., and Iverson, R., eds., Prediction in geomorphology: Washington, D.C., American Geophysical Union, Geophysical Monograph 135, p. 103–132.

Fleming, R.W., and Johnson, A.M., 1975, Rates of seasonal creep of silty clay soil: Engineering Geology Quarterly Journal, v. 8, p. 1–29.

Furbish, D.J., 2003, Using the dynamically coupled behavior of land-surface geometry and soil thickness in developing and testing hillslope evolution models, *in* Wilcock, P., and Iverson, R., eds., Prediction in geomorphology: American Geophysical Union Geophysical Monograph 135, p. 169–182.

Gabet, E.J., 2000, Gopher bioturbation: Field evidence for nonlinear hillslope diffusion: Earth Surface Processes and Landforms, v. 25, p. 1419–1428.

Gabet, E.J., 2003, Sediment transport by dry ravel: Journal of Geophysical Research, v. 108, no. B1, doi: 10.1029/2001JB001686.

Galloway, A.J., 1977, Geology of the Point Reyes Peninsula, Marin County, California: Sacramento, California Division of Mines and Geology, p. 72.

Heimsath, A.M., Dietrich, W.E., Nishiizumi, K., and Finkel, R.C., 1997, The soil production function and landscape equilibrium: Nature, v. 388, p. 358–361.

Heimsath, A.M., Dietrich, W.E., Nishiizumi, K., and Finkel, R.C., 1999, Cosmogenic nuclides, topography, and the spatial variation of soil depth: Geomorphology, v. 27, p. 151–172.

Heimsath, A.M., Chappell, J., Dietrich, W.E., Nishiizumi, K., and Finkel, R.C., 2000, Soil production on a retreating escarpment in southeastern Australia: Geology, v. 28, p. 787–790.

Heimsath, A.M., Chappell, J., Spooner, N.A., and Questiaux, D.G., 2002, Creeping soil: Geology, v. 30, p. 111–114.

Matsuoka, N., and Moriwaki, K., 1992, Frost heave and creep in the Sor Rondane Mountains, Antartica: Arctic and Alpine Research, v. 24, p. 271–280.

McKean, J.A., Dietrich, W.E., Finkel, R.C., Southon, J.R., and Caffee, M.W., 1993, Quantification of soil production and downslope creep rates from cosmogenic ^{10}Be accumulations on a hillslope profile: Geology, v. 21, p. 343–346.

Reneau, S.L., 1988, Depositional and erosional history of hollows: Application to landslide location and frequency, long-term erosion rates, and the effects of climatic change [Ph.D. thesis]: Berkeley, University of California, 328 p.

Roering, J.J., 2004, Soil creep and convex-upward velocity profiles: Theoretical and experimental investigation of disturbance-driven sediment transport on hillslopes: Earth Surface Processes and Landforms, v. 29, p. 1597–1612.

Roering, J.J., and Gerber, M., 2005, Fire and the evolution of steep, soil-mantled landscapes: Geology, v. 33, p. 349–352.

Roering, J.J., Kirchner, J.W., and Dietrich, W.E., 1999, Evidence for non-linear, diffusive sediment transport on hillslopes and implications for landscape morphology: Water Resources Research, v. 35, p. 853–870.

Roering, J.J., Kirchner, J.W., Sklar, L.S., and Dietrich, W.E., 2001, Hillslope evolution by nonlinear creep and landsliding: An experimental study: Geology, v. 29, p. 143–146.

Roering, J.J., Almond, P., Tonkin, P., and McKean, J., 2002, Soil transport driven by biological processes over millenial time scales: Geology, v. 30, p. 1115–1118.

Manuscript received 18 May 2005
Revised manuscript received 12 August 2005
Manuscript accepted 15 August 2005

Printed in USA

APPENDIX: Obtaining Soil Flux from Integration of the Soil Production Rate

PRINCIPLES AND PRACTICE

The magnitude of the soil flux $h\bar{\mathbf{q}}$ [$L^2\ t^{-1}$] can be estimated from downslope integration of the local soil production rate p_η [$L\ t^{-1}$] between two arbitrarily curved "flow lines" of downslope soil motion. Here we first describe this integration as applied to sites at Nunnock River, Point Reyes and Tennessee Valley. We then examine possible sources of error in our estimates of soil flux arising from the numerical integration and from the assumption that the rate of change in soil storage is negligible.

To illustrate the idea behind the downslope integration, first consider two soil transport flow lines that are parallel and straight and separated by a uniform contour distance B. Let x denote a horizontal axis that is positive in the downslope direction. The z-axis is vertical and positive upward. Neglecting horizontal tectonic motion the vertically integrated equation of mass conservation is:

$$\frac{\partial}{\partial x}\left(Bh\bar{q}_x\right) + \frac{\partial}{\partial t}\left(Bh\bar{c}\right) + Bc_\eta p_\eta = 0, \tag{A.1}$$

where $\bar{q}_x$ is the vertically averaged soil flux density parallel to x, h is the soil thickness, $\bar{c}$ is the vertically averaged soil concentration, c_η is the soil concentration at the base of the soil, p_η is the rate of soil production, and t is time. Note also that, although B could be removed from (A.1), we retain it here for illustration. Integrating this with respect to x from the divide ($x = 0$) to a position $x = X$,

$$Q(X,t) = -B\int_0^X \frac{\partial}{\partial t}(h\bar{c})\,dx - B\int_0^X c_\eta p_\eta\,dx, \tag{A.2}$$

which illustrates that the total soil flux $Q(X)$ [$L^3\ t^{-1}$] at position $x = X$, that is $Q(X) = Bh\bar{q}_x|_X$, obtains by integrating the unsteady term and the soil production rate upslope of X. In the case of steady soil thickness h, and uniform and constant concentrations $\bar{c}$ and c_η, this reduces to

$$Q(X) = -Bc_\eta\int_0^X p_\eta\,dx. \tag{A.3}$$

If the production rate p_η is uniform, then the soil flux $Q(X)$ increases linearly with X. Note that the first integral quantity in (A.2) is equivalent to integrating the local rate of change in soil storage, $\partial(h\bar{c})/\partial t$, over the area $A(X) = BX$. Similarly, the second integral quantity in (A.2) and the integral quantity in (A.3) are equivalent to integrating the local soil production rate over the area $A(X) = BX$. Also note that the soil flux per unit contour distance at position X is $Q(X)/B$. The formulation above can be generalized to a curvilinear or radial coordinate system (Furbish, unpublished notes), although it suffices here to proceed to a simpler formulation that builds on these points.

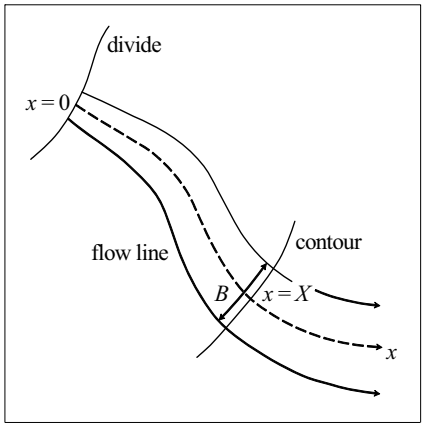

Figure A1. Curvilinear coordinate system; flow lines normal to contours.

Consider two soil transport flow lines that are everywhere normal to elevation contours (Fig. A1). For convenience we now let x denote a curvilinear downslope coordinate centered

between the two flow lines with origin ($x = 0$) at the upslope divide. At any coordinate position x there is an arbitrarily curved elevation contour segment, locally normal to x, with length B between the two flow lines. Thus, $B = B(x)$.

The total soil flux Q [L^3 t^{-1}] passing a given contour segment at position $x = X$ must equal the total rate of soil production, minus the rate of change in storage, upslope of the segment between the flow lines. Thus,

$$Q(X,t) = -\int_{A(X)} c_\eta p_\eta \, dA - \int_{A(X)} \frac{\partial}{\partial t}(h\bar{c}) \, dA , \tag{A.4}$$

indicating that $Q(X, t)$ is obtained by simply integrating the local production rate and the rate of change in soil storage over the area $A(X)$ upslope of $x = X$.

As described in the next section, we assume that the soil storage term in (A.4) is negligible relative to the other terms whence,

$$Q(X) \approx -c_\eta \int_{A(X)} p_\eta \, dA , \tag{A.5}$$

where c_η is assumed to be uniform. With square brackets denoting an average, the magnitude of the soil flux per unit contour distance at position $x = X$ is then estimated as an average over $B(X)$, namely $[h\bar{q}_x]|_X = Q(X)/B(X)$, which is the value that we report in the text.

The numerical integration of (A.5) is performed as follows. Voronoi polygons are constructed for soil thickness measurements within and near the total area $A(X)$. Let a_i denote the subarea of the ith polygon falling within $A(X)$ such that $A(X) = \sum a_i$. Then assuming the local soil production rate $p_\eta = -P\exp(-h/\gamma)$,

$$Q(X) \approx c_\eta P \sum_i^N a_i \exp(-h_i/\gamma) , \tag{A.6}$$

where N is the total number of polygon subareas. The importance of constructing Voronoi polygons is that this procedure objectively weights each local production rate (obtained from measured soil thickness) in proportion to its relative areal (Voronoi) coverage within $A(X)$.

We also note that reported slopes are averages obtained at position X. That is, we estimated local slopes for two to seven locations along B (depending on its length), then averaged these to obtain $S(X)$. The significance of this is that plots involving flux, slope and the depth-slope product are based on averages over $B(X)$ rather than representing "local" values.

TRANSIENT SOIL STORAGE

Nonuniform soil thicknesses on the hillslopes suggest that transient soil storage is non-zero. Nonetheless we suggest that the storage term in (A.4) is significantly smaller than the other terms, with the implication that (A.5) is an adequate estimate of the soil flux.

Under steady-state conditions, where either uplift is balanced by stream incision at the lower hillslope boundary or the land-surface is lowering uniformly, the storage term in (A.4) is zero (for constant $\bar{c}$). Changes in storage are thus related either to changes in the lower boundary condition wherein effects of this condition are propagated upslope, or to changes in the soil transport rate due to a change in the transport coefficient (or diffusivity), or both. The sites were selected to avoid

complications related to possible changes in transport processes, so here we focus on the magnitude of soil storage related to changes in the lower boundary condition. The downslope thickening soils at the field sites in particular are consistent with cessation of stream downcutting, whence soils thicken with time, and this thickening slowly propagates upslope.

Assuming momentarily that the soil flux is proportional to slope, namely $Q(X) = -BDS$ where D [L^2 t^{-1}]is a diffusivity, then with uniform c_η and constant $\bar{c}$, (A.4) integrates to

$$BDS(X,t) = c_\eta A\langle p_\eta\rangle + \bar{c}A\frac{\partial\langle h\rangle}{\partial t}, \tag{A.7}$$

where chevron brackets denote that the quantity is averaged over the area A. Under steady conditions this reduces to

$$BDS(X) = c_\eta A\langle p_\eta\rangle. \tag{A.8}$$

The terms in (A.7) can be directly scaled to evaluate their relative magnitudes. To clarify the physical basis for this scaling, however, we consider the rate of change of these terms in response to a change in the lower boundary condition.

Envision a change in the transport rate BDS during a small interval dt, following a steady state condition at time t. Expanding (A.7) as a Taylor series about t,

$$BDS(X,t+\mathrm{d}t) = BDS(X,t) + BD\frac{\partial S}{\partial t}\mathrm{d}t$$

$$= c_\eta A\langle p_\eta\rangle(t) + c_\eta A\frac{\partial\langle p_\eta\rangle}{\partial t}\mathrm{d}t + \bar{c}A\frac{\partial^2\langle h\rangle}{\partial t^2}\mathrm{d}t + \mathrm{O}[(\mathrm{d}t)^2]. \tag{A.9}$$

Thus, the new transport rate at time t + dt involves the "old" steady-state balance at time t; and the change in the transport rate is balanced by changes in production or storage, or both. Thus, to clarify when the storage term can be neglected, it suffices to show when the term involving the second derivative is small relative to terms involving first derivatives. More simply, the rate of change of (A.7) is

$$BD\frac{\partial S}{\partial t} = c_\eta A\frac{\partial\langle p_\eta\rangle}{\partial t} + \bar{c}A\frac{\partial^2\langle h\rangle}{\partial t^2}, \tag{A.10}$$

which may be viewed as a measure of the extent to which a change in soil production is accommodated by a change in transport versus being partitioned into storage.

Let $S = \partial\zeta/\partial x$, where ζ is the land-surface elevation. Then noting that $\partial\langle p_\eta\rangle/\partial t = \partial\langle -P\exp(-h/\gamma)\rangle/\partial t \approx (1/\tau)\partial\langle h\rangle/\partial t$, where $\tau = \gamma/\langle p_\eta\rangle$ is a measure of the mean soil residence time,

$$BD\frac{\partial}{\partial t}\left(\frac{\partial\zeta}{\partial x}\right) = \frac{c_\eta A}{\tau}\frac{\partial\langle h\rangle}{\partial t} + \bar{c}A\frac{\partial^2\langle h\rangle}{\partial t^2}. \tag{A.11}$$

The slope and the soil thickness must change over the same timescale T in response to a change in the lower boundary condition. We thus define the following dimensionless quantities denoted by a circumflex:

$$\zeta = \gamma\hat{\zeta}, \quad \langle h\rangle = \gamma\hat{h}, \quad x = \lambda\hat{x} \text{ and } t = T\hat{t}. \tag{A.12}$$

Substituting these first into (A.8) obtains

$$\frac{\partial \hat{\zeta}}{\partial \hat{x}}\Big|_{x=X} = c_\eta \frac{T^*}{\tau}, \tag{A.13}$$

where $T^* = \lambda A/BD$ is like a relaxation timescale. (Note that, in the case of parallel, straight flow lines, $A = BX$, whence $T^* = \lambda X/D$.) Moreover, this steady-state case requires that $T^* \sim \tau$.

Turning to (A.11),

$$\frac{\tau}{T^*}\frac{\partial}{\partial x}\left(\frac{\partial \hat{\zeta}}{\partial \hat{t}}\right)\Big|_{x=X} = c_\eta \frac{\partial \hat{h}}{\partial \hat{t}} + \bar{c}\frac{\tau}{T}\frac{\partial^2 \hat{h}}{\partial \hat{t}^2}, \tag{A.14}$$

which indicates that the last term can be neglected if $\tau \sim T^* \ll T$. Qualitatively, inasmuch as transport depends on land-surface slope, any effect on transport due to a change in the lower boundary condition is felt through changes in slope that propagate upslope. For a relaxing hillsope, a change in transport rate (i.e. a change in slope) generally involves a change in soil thickness (and a concomitant change in soil production), which implies a change in storage. Nonetheless, inasmuch as changes in soil thickness occur over a timescale that is much longer than the mean soil residence time, soil production remains essentially balanced by transport.

For completeness we substitute (A.12) into (A.7) with $\tau \sim T^* = \lambda A/BD$ to obtain:

$$\frac{\partial \hat{\zeta}}{\partial \hat{x}}\Big|_{x=X} - c_\eta = \bar{c}\frac{\tau}{T}\frac{\partial \hat{h}}{\partial \hat{t}} = \bar{c}\frac{\lambda A}{BDT}\frac{\partial \hat{h}}{\partial \hat{t}}. \tag{A.15}$$

Based on the scaling quantities adopted in (A.12) and applied in (A.15), the timescale T may be interpreted as the time that it takes to accumulate a soil thickness equal to $\gamma \sim h$. In the absence of transport — assuming that all production goes into storage — then $T \sim \tau$, typically on the order of several thousand years, the shortest possible value of T. Numerical simulations of relaxing hillslopes suggest, however, that to accumulate (excess) soil thicknesses equal to $\gamma \sim h$ requires periods approaching the relaxation time of the hillslope, $T_R \sim L^2/D$, where L is the hillslope length (Furbish, 2003; Furbish and Dietrich, in prep.).

The scaling in (A.15) also reveals important consequences of land-surface slope and gradient. The lengthscale λ may be interpreted as the distance over which the land-surface elevation changes by an amount $\Delta\zeta \sim \gamma$. Thus, as λ increases (slope decreases), the timescale T^* increases such that the magnitude of the storage term increases. This merely reflects that, with decreasing slope and therefore decreasing soil throughput, the mean residence time increases. In addition, for given area A, a small ratio A/B coincides with diverging flow lines, whereas a large ratio A/B coincides with converging flow lines. Thus, the significance of the storage term decreases with increasing divergence of the lines, whereas this term may become increasingly important with converging flow lines.

A similar scaling can readily be applied with the assumption that the soil flux is proportional to the product of soil thickness and land-surface slope, namely $Q(X) = -BK\langle h\rangle S$ where K [L t^{-1}] is a transport coefficient. Using (A12) with $\tau \sim T^* = \lambda A/BK\gamma$ we obtain:

$$\hat{h}\frac{\partial \hat{\zeta}}{\partial \hat{x}}\Big|_{x=X} - c_\eta = \bar{c}\frac{\tau}{T}\frac{\partial \hat{h}}{\partial \hat{t}} = \bar{c}\frac{\lambda A}{BK\gamma T}\frac{\partial \hat{h}}{\partial \hat{t}}. \tag{A.16}$$

Comparing this with (A.15) it is apparent that conclusions regarding the importance of the storage term are the same as those outlined above.

SPURIOUS CORRELATION BETWEEN FLUX, SLOPE AND THICKNESS

If the hypothesis that soil flux is linearly proportional to land-surface slope is correct, then a plot of flux $[h\overline{\boldsymbol{q}}_{\boldsymbol{x}}]|_X = Q(X)/B(X)$ versus slope $S(X)$ should in principle exhibit a linear trend with zero intercept and slope equal to the diffusivity D. Similarly, if the hypothesis that soil flux is proportional to the product of soil thickness and land-surface slope is correct, then a plot of flux $[h\overline{\boldsymbol{q}}_{\boldsymbol{x}}]|_X$ versus the product $h(X)S(X)$ should exhibit a linear trend with zero intercept and slope equal to the transport coefficient K (Fig. 3A). However, as an integrated quantity, th soil flux, see (A.5), must generally increase with downslope distance. Moreover, both slope and thickness generally increase downslope at the field sites. This means that plots of flux versus slope, or flux versus the product of thickness and slope, may exhibit spurious (positive) correlations, and therefore do not represent a rigorous "test" of the two hypotheses. For this reason we consider plots involving the ratios $[h\overline{\boldsymbol{q}}_{\boldsymbol{x}}]|_X/S(X)$ and $[h\overline{\boldsymbol{q}}_{\boldsymbol{x}}]|_X/h(X)S(X)$ versus distance X (Figure 3B). The effect of this is to remove correlations among flux, slope and thickness. For the data to be consistent with one of the transport hypotheses, the trends in these plots should be flat, at a value equal to either D or K. See Data Repository Figures A2 and A3, below, for plots of flux versus gradient and flux/gradient.

REFERENCES CITED

Furbish, D. J. 2003. Using the dynamically coupled behavior of land-surface geometry and soil thickness in developing and testing hillslope evolution models. *in* P. Wilcock and R. Iverson (Eds.), *Prediction in Geomorphology*, American Geophysical Union, Geophysical Monograph 135, Washington, D.C., 169-181.

Furbish, D. J. and Dietrich, W. E. On the use of a diffusion-like equation to describe hillslope evolution: 1. Formulation and scaling. (*in preparation*)

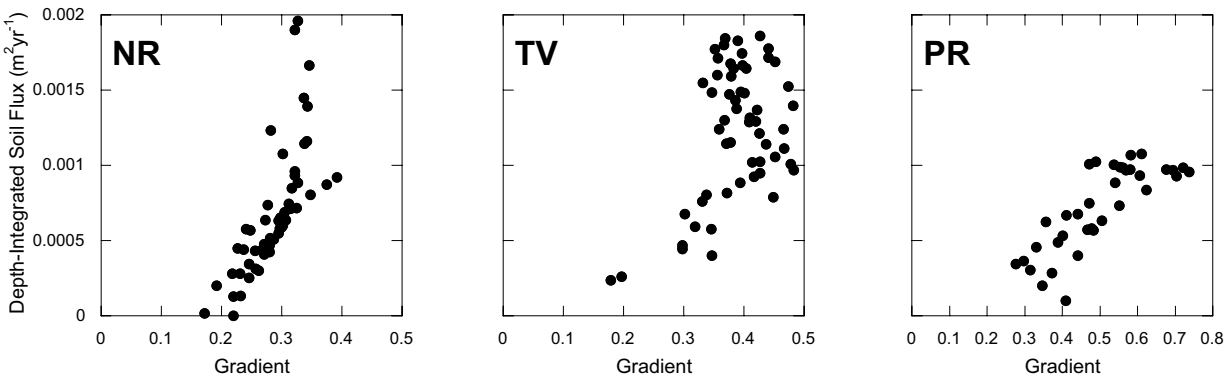

Data Repository Figure A2: Depth-integrated soil flux used in Figure 3 in text (calculated as described above) per unit contour length (m^2yr^{-1}) versus the gradient for all field sites.
For data to fit the linear slope-dependent transport law both a linear increase of flux with gradient, as well as an intercept with the origin (i.e. zero flux at zero slope) are required.
NR-Nunnock River; TV-Tennessee Valley; PR-Point Reyes.

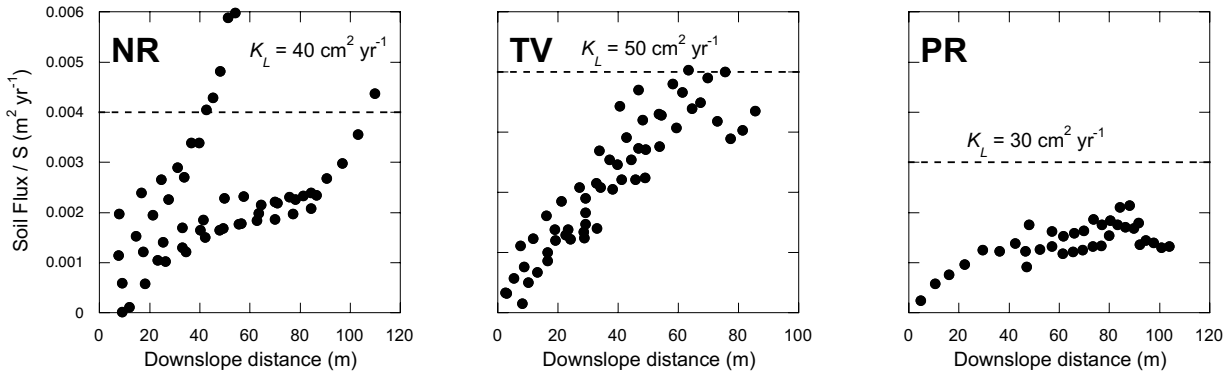

Data Repository Figure A3: Depth-integrated flux divided by gradient versus downslope distance. K_L value is dashed line independently determined by several different studies: NR value from Heimsath et al. (2000); TV value from Reneau (1988), used in Dietrich et al. (1995) and Heimsath et al. (1997, 1999); PR value from Reneau (1988).
Used in a similar way to Figure 3B in the text, these data would support a linear slope-dependent transport law if the data were homoscedastic about the transport coefficient plotted as the dashed line for each site.
NR-Nunnock River; TV-Tennessee Valley; PR-Point Reyes.